Secondary “distal lahars” after the ~4.2 ka BP Cerro Blanco Plinian eruption, Argentina: implications for source parameter estimation and volcanic hazard assessment

Walter Báez[1,2], Shanaka de Silva[1]*

[1] *College of Earth, Ocean, and Atmospheric Sciences, Oregon State University, Corvallis, OR 97331-5503, United States of America*
[2] *IBIGEO (UNSa – CONICET), Av. Bolivia 5150, A4400FVY Salta, Argentina*
* Corresponding Author

geowbsalta@gmail.com/Shanaka.deSilva@oregonstate.edu

Abstract

Mass flows can remobilize ash-rich tephra deposited tens to hundreds of kilometers from its source during large Plinian eruptions, forming secondary “distal lahars”. Despite its significance, this process has received little attention, particularly from a hazard perspective. Recognizing remobilization processes in distal tephra is crucial for accurately estimating eruptive source parameters (e.g., volume) from pyroclastic deposits and ensuring the reliable use of these deposits for tephrochronological purposes. In this study, we present a facies analysis of distal tephra deposits associated with the ~4.2 ka BP Cerro Blanco Plinian caldera-forming eruption (Northwest Argentina). Although previous studies have classified this eruption as a Volcanic Explosivity Index 7 event, many distal deposits appear to have been remobilized, raising questions about that classification. Our observations indicate that secondary “distal lahars” were the dominant remobilization mechanism in distal areas in the aftermath of the eruption. These findings have implications for both hazard assessment and the estimated volume of the Cerro Blanco eruption, which may warrant revision.

Keywords: Tephra remobilization, Tephrochronology, Eruption volume, Volcanic hazard, Cerro Blanco

“Lahares distales” secundarios tras la erupción Pliniana del Cerro Blanco, Argentina (~4,2 ka AP): implicancias para la estimación de parámetros fuente y la evaluación del peligro volcánico. Los flujos de masa pueden removilizar ceniza volcánica depositada a decenas o cientos de kilómetros de su fuente durante grandes erupciones plinianas, formando "lahares distales" secundarios. A pesar de su importancia, este proceso ha recibido escasa atención, especialmente desde una perspectiva de evaluación de peligros volcánicos. El reconocimiento de los procesos de removilización en tefras distales es crucial para estimar con precisión los parámetros eruptivos de la fuente (e.g., volumen) a partir de los depósitos piroclásticos, así como para asegurar el uso confiable de estos depósitos con fines tefrocronológicos. En este estudio, se presenta un análisis de facies de los depósitos de tefra distales asociados con la erupción pliniana del Cerro Blanco (~4,2 ka AP, Noroeste de Argentina). Estudios previos han clasificado esta erupción como un evento con un Índice de Explosividad Volcánica 7; sin embargo, muchos de los depósitos distales parecen haber experimentado removilización, lo que ha generado un debate sobre esa clasificación. Los resultados expuestos aquí indican que los "lahares distales" secundarios fueron el principal mecanismo de removilización en áreas alejadas del volcán tras la erupción. Esto presenta implicancias tanto para la evaluación del peligro volcánico como para la estimación del volumen de la erupción del Cerro Blanco, lo cual podría requerir una actualización.

Palabras clave: Removilización de tefra, Tefrocronología, Volumen eruptivo, Peligros volcánicos, Cerro Blanco

1. Introduction

Plinian eruptions, with Volcanic Explosivity Index (VEI) values ranging from 4 to 8, are among the most powerful natural hazards, capable of causing massive economic and human losses, even on a global scale (e.g., Robock, 2000; Newhall et al., 2018). These eruptions produce buoyant, vertically directed eruptive columns that can rise tens of kilometers because of sustained, high-mass eruption rates at the vent (Wilson et al., 1980; Cioni et al., 2015). At its maximum height, the eruptive column spreads laterally, forming an umbrella cloud that can be transported thousands of kilometers by wind (Wilson et al., 1980; Cioni et al., 2015). Tephra deposits from Plinian eruptions typically consist of thick blankets of well-sorted, pumice-rich lapilli in proximal areas, transitioning downwind into ash-rich beds that cover vast regions (Walker, 1981; Giordano et al., 2024).

Beyond the immediate impacts of tephra dispersion and fallout during Plinian eruptions, such as threats to public health, disruption of critical infrastructure, aviation hazards, and impacts on crop and livestock production (Jenkins et al., 2015), tephra remobilization by wind or water can cause severe, long-lasting effects that persist for decades to even millennia (e.g., Willson et al., 2011; Mingari et al., 2017; Paredes-Mariño et al., 2022). In particular, torrential rains can remobilize tephra accumulated on the volcano's flanks, triggering secondary lahars (Smith and Lowe, 1991; Vallance, 2005, 2024; Harpel et al., 2011; Manville et al., 2013; Vallance and Iverson, 2015). While this process has been extensively studied, mainly due to its significance during major historical eruptions (e.g., Pierson et al., 1990, 1992; Janda et al., 1996; Lavigne et al., 2000; Castruccio et al., 2010), rain-driven remobilization of ash-rich tephra deposited tens to hundreds of kilometers from the volcano months to years following large Plinian eruptions has received significantly less attention, particularly from a hazard perspective (e.g., Córdoba et al., 2015). We refer to these remobilized distal deposits as secondary "distal lahars" (Baumann et al., 2018, 2020; Mulas et al., 2019; Buckland et al., 2020; Cortés-Jiménez, 2020; Di Vito et al., 2023; Losano et al., 2024).

In the Argentine Andes of South America, the Cerro Blanco eruption was a large rhyolitic, caldera-forming Plinian event that occurred approximately 4.2 ka BP. It produced widely dispersed fallout deposits and pyroclastic density currents (PDCs) that inundated surrounding valleys up to 35 km from the vent (Báez et al., 2015, 2020a; Fernández-Turiel et al., 2019). Current estimates indicate that the Cerro Blanco eruption was a VEI 7 event, with a dense-rock equivalent eruption volume of 83.5 km^3 (Fernández-Turiel et al., 2019). Due to its size, the eruption blanketed a vast portion of northern Argentina with ash (Fernández-Turiel et al., 2019; Boretto et al., 2021) and likely had a significant impact on Middle Holocene human occupation in northwestern Argentina (Montero-López et al., 2009; Ratto, 2013; Carbonelli et al., 2022). Some studies, however, indicate that distal tephra outcrops associated with Cerro Blanco show evidence of local remobilization, potentially affecting the reliability of volume and VEI estimates (Sampietro-Vattuone et al., 2020; Báez et al., 2020a).

To date, no detailed sedimentological study has assessed whether these distal tephras are primary or secondary in origin, an essential step for deriving accurate eruptive source parameters from pyroclastic deposits. In this study, we address that knowledge gap through a facies analysis of distal Cerro Blanco tephra deposits in the Tafí Valley area (Tucumán Province), ~200 km east of the source. Our primary objective is to investigate the character (primary, remobilized, or reworked) of these distal ashes and rigorously assess their volcanological and tephrochronological implications.

2. Geological setting

2.1. Cerro Blanco Volcanic Complex

The Cerro Blanco Volcanic Complex (CBVC) is a nested caldera complex located on the southern edge of the Central Volcanic Zone of the Andes, within the San Buenaventura Volcanic Chain (Fig. 1A, B) (Seggiaro et al., 2006; Montero-López et al., 2010; Báez et al., 2015). Its volcanic products, all rhyolitic to rhyodacitic in composition, span from the Late Pleistocene to the Holocene (Montero-López et al., 2010; Báez et al., 2015; de Silva et al., 2022). The CBVC comprises PDCs and fall deposits associated with two major Plinian caldera-forming eruptions (Báez et al., 2015; Fig. 1C).

The oldest of these eruptions produced the Campo de la Piedra Pómez ignimbrite and its associated fallout deposits (Báez et al., 2020b, 2025). The Campo de la Piedra Pómez eruption was a VEI ≥6 event which began with a sustained Plinian phase, during which partial column collapse generated small, highly mobile PDCs (Báez et al., 2025). Caldera collapse followed this stage and involved a mixed eruptive style that combined pyroclastic fountaining (boiling-over) from fissure-like vents with a convective Plinian column. As the eruption progressed, Plinian activity gradually ceased. Zircon Double Dating indicates an age of ~30 ka for the Campo de la Piedra Pómez eruption (Báez et al., 2025).

The youngest major eruption at the CBVC was the ~4.2 ka BP (calibrated ^{14}C age) Cerro Blanco caldera-forming event, classified as a VEI 7 eruption (Fernández-Turiel et al., 2019). This eruption involved the simultaneous development of convective and collapsing column dynamics, generating widely dispersed fallout deposits and extensive PDCs (Báez et al., 2020a). Holocene activity at the CBVC also includes smaller-scale explosive eruptions, as well as several pre- and post-caldera lava domes with associated block-and-ash flows (Montero-López et al., 2010; Báez et al., 2015, 2017). The system remains active today, as evidenced by geothermal activity (Chiodi et al., 2019; Lamberti et al., 2021) and ongoing subsidence (Henderson and Pritchard, 2013; Vélez et al., 2021).

2.2. Tafí Valley

The Tafí Valley is located in northwestern Argentina (Tucumán Province), approximately 200 km east of the CBVC (Fig. 1B). It is one of the many semi-arid intermontane valleys situated east of the southern Puna Plateau, along the Eastern Cordillera and the Sierras Pampeanas (Fig. 1B). The topographic highs in the Tafí Valley area consist of granite and metamorphic rocks of Precambrian-lower Paleozoic age (Ruiz Huidobro, 1972; Toselli et al., 1978; Galván, 1981) and minor Paleogene deposits (González, 1997). The valley's Holocene infill includes several intermountain sequences, at least five of which are ash layers, encompassing the ~4.2 ka BP Cerro Blanco eruption deposit (Sampietro-Vattuone et al., 2020). Holocene sedimentation in the Tafí Valley reflects a succession of aggradational episodes punctuated by periods of fluvial incision, which together define four distinct stratigraphic units (Sampietro-Vattuone and Peña-Monné, 2019). The oldest unit (H1) records Early Holocene (~13-4.2 ka BP) landscape evolution and is mainly preserved as colluvial and other slope-related deposits. A Late Holocene (~4.2-0.6 ka BP) interval of enhanced sediment accumulation (H2) succeeded this unit, during which sedimentation extended across hillslopes and fluvial environments, producing terraces and alluvial fan deposits. More restricted fluvial and alluvial bodies assigned to units H3 and H4 record subsequent sedimentary activity and are confined to incised channels that truncate the older deposits. These youngest units document depositional processes operating from ~0.6 ka BP up to the present day (Sampietro-Vattuone and Peña-Monné, 2019).

3. Methodology

3.1 General approach

We conducted a detailed analysis of lateral facies variations on the eastern side of the Tafí Valley along a transect following the drainage network (Fig. 2A, B). We selected this area because it provides exceptional exposures of Holocene ash layers and the highest tephrochronological resolution in northwestern Argentina (e.g., Hermanns and Schellenberger, 2008; Fernández-Turiel et al., 2019; Sampietro-Vattuone et al., 2020; Báez et al., 2024). We examined three Holocene sections in detail where previous studies identified tephras associated with the Cerro Blanco eruption (Fig. 2B). Two of the studied sections contain the so-called "double" Cerro Blanco tephra: two geochemically identical yet stratigraphically distinct ash layers, which previous studies interpreted as evidence of two large Holocene eruptions from the CBVC (Hermanns et al., 2000, 2006; Hermanns and Schellenberger, 2008; Sampietro-Vattuone et al., 2020; Báez et al., 2024). This study does not aim to evaluate that hypothesis but rather to identify remobilization processes within these deposits.

3.2 Methods and terminology

We use the terms "primary" and "secondary volcaniclastic deposits" following the definitions proposed by Sohn and Sohn (2019) and Di Capua et al. (2023). Primary volcaniclastic deposits are formed when particles are generated, transported, and emplaced directly by volcanic processes. In contrast, secondary volcaniclastic deposits consist of particles that originate from volcanic activity but are transported and deposited by non-volcanic mechanisms such as alluvial, fluvial, and/or aeolian processes. We also adopt the term "remobilized pyroclastic deposits" as a synonym for secondary volcaniclastic deposits, following the usage by Petrinovic and D'Elia (2018). Additionally, we use the term "volcanic epiclastic deposits" to refer to deposits derived from the weathering and/or erosion of volcanic materials, in which particles are transported and redeposited by non-volcanic processes (Di Capua et al., 2023). This usage implies the reworking of volcanic material (e.g., Petrinovic and D'Elia, 2018). In this study, we consider remobilization and reworking to be distinct processes and therefore do not use the terms interchangeably (e.g., Petrinovic and D'Elia, 2018).

We describe the distal tephras in the field using a non-genetic approach, focusing on thickness, color, grain size, componentry, homogeneity, contacts with underlying and overlying deposits, and internal structures. We adopted the nomenclature proposed by

Branney and Kokelaar (2002) to classify each facies as they mostly consist of well-preserved pyroclastic material. However, its application here is inherently interpretive since the studied sections contain both primary deposits and syn-eruptive and/or early post-eruptive remobilized pyroclastic deposits, and not primary deposits only. In addition, because the primary and remobilized pyroclastic deposits described here share most of their general sedimentological characteristics (e.g., componentry, texture, grain size), we describe all facies using nomenclature commonly applied to pyroclastic deposits (e.g., Froese et al., 2006).

We use the term "mass flow" as a general descriptor for any gravity-driven downslope movement of material (e.g., Iverson, 2003). These flows encompass a spectrum of phenomena involving mixtures of particles and interstitial fluid, ranging from dilute flows to more concentrated forms such as granular avalanches and debris flows (Iverson, 2003).

Lapilli and ash grain size subdivisions follow White and Houghton (2006). We collected distal tephra samples for grain size and componentry analyses while carefully avoiding contamination from adjacent layers. We manually sieved the samples at 1ϕ intervals to determine grain size distributions and processed the resulting data using the Folk and Ward (1957) method implemented in GRADISTAT (Blott and Pye, 2001). We estimated the componentry of each size fraction using a binocular microscope. We further characterized glass-shard textures using images acquired with a JEOL scanning electron microscope at the Scanning Electron Microscopy and Microanalysis Laboratory, National University of Salta, Argentina. For comparison, we also obtained scanning electron microscope images of pyroclastic particles from a pyroclast-rich active dune located near the study area (see location in figure 1B).

4. Results and interpretation

We identified three main pyroclastic facies in the Holocene sections of the Tafí Valley, which we describe and interpret in detail below.

Massive Tuff (mT) facies*:* corresponds to structureless, fine-ash-rich deposits composed predominantly of vitric shards (>90%) and minor crystal fragments (<10%) (Fig. 2C). This facies occurs as tabular to lenticular bodies with undulating but sharp lower and upper contacts (Fig. 3A), and we observed it only in the basin catchment zone, associated with peatland environments forming <50 cm-thick monofacial levels. Previous studies have described similar facies elsewhere within the Tafí Valley but always associated with low-energy environments (e.g., Hermanns and Schellenberger, 2008). Bioturbation is quite common. Vitric shards display variable shapes: cuspate, platy, and blocky, and show good preservation of their primary morphology, as do the micro-pumice fragments (Fig. 2D, E). Crystals include quartz, plagioclase, and large (<2 mm) biotite grains. The absence of internal structures and epiclastic contamination, both indicative of remobilization, supports the interpretation of the *mT* facies as a primary fallout deposit.

Thin-bedded Tuff (tbT) facies*:* corresponds to thin-bedded, fine-ash-rich deposits composed predominantly of vitric shards (>90%), crystals (~5%), and some accidental lithic clasts (<5%) (Fig. 2C). It is the most developed facies in the lower parts of the basin and always occurs together with the *tsT* facies (see below), forming tabular to extended lenticular bodies (local valley pond or channelized morphologies) (Fig. 2B). It presents sharp lower and upper contacts (Fig. 3B, C). The bulk grain size distribution and componentry of the *tbT* facies are quite similar to those of the *mT* facies (Fig. 2C), but internally, the *tbT* facies exhibits thin bedding generated by alternating coarse and fine ash layers (Fig. 4A-C). Truncations of individual layers are rare, and low-angle cross-bedding is absent. As with the *mT* facies, vitric shards in the *tbT* facies display variable shapes, such as cuspate, platy, and blocky. Micro-pumices are also present, and, as with the vitric shards, the preservation of their primary morphologies is good (Fig. 2D, E). Accidental lithic clasts can reach 3-4 cm, making them outsized clasts when compared to the bulk granulometry of the deposit (Fig. 4A). The presence of these outsized clasts, along with the absence of cross-stratification or significant bed truncations, is consistent with a high-strength debris flow regime. However, we interpret the alternation of fine and coarse ash layers as the result of rapid deposition from a hyperconcentrated flow, without the development of high-relief bedforms, or from aggrading deposition within a bipartite traction carpet related to density-stratified flows (Sohn, 1997).

Thin-stratified Tuff (tsT) facies*:* correspond to thin-stratified, coarse ash-rich deposits formed predominantly by vitric shards (~70-80%), crystals (~25-15%), and lithic clasts (~5%) (Fig. 2C). Internally, this facies exhibits alternating, parallel, thin beds of coarse ash/scarce lapilli and fine to coarse ash (Fig. 4A, B). Truncation of individual layers, planar cross-stratification, and load-driven soft deformation are also common (Fig. 4B, D, E). The *tsT* facies is markedly different from previous facies, both in grain size distribution and componentry (Fig. 2C). It is fine-ash poor and has a much higher presence of crystals and lithic clasts than the *mT* and *tbT* facies (Fig. 2C). However, glass shards and micro-pumices have a similar morphology and degree of preservation when compared to those from the *mT* and *tbT* facies (Fig. 2D, E). Lithic clasts are mainly basement rocks similar to those outcropping in the Tafí Valley region. Crystals include quartz, plagioclase, and large biotite (up to 2 mm). The *tsT* facies always occurs associated with the *tbT* facies in the lower parts of the basin. Specifically, the *tsT* facies systematically develops at the base of the *tbT* facies, while it only occasionally appears interbedded with the *tbT* facies or at its top (Figs. 2B and 5). This facies association presents progressive downstream increase in thickness and epiclastic contribution (Fig. 2A, B). For instance, at the CBT5 section the *tsT/tbT* facies association is ~50 cm thick, whereas at CBT7 (~8 km downstream) it thickens to up to 2 m. It is worth noting that we also observed this increase in thickness towards the main channels of the individual sub-basins in the upper reaches of the Tafí Valley (Sampietro-Vattuone and Peña-Monné, 2016). The *tsT/tbT* facies association occurs as tabular bodies with sharp lower and upper contacts (Fig. 4A) or as extended lenticular bodies (local valley pond or channelized morphologies). Beyond the Tafí Valley area, previous studies also recognized this facies association at ~70-90 km east of the CBVC (e.g., Cuesta de Randolfo site; Figs. 1B and 5).

The *tsT* facies, characterized by fine-ash-poor grain size and planar cross-stratification, indicates an increase in water content with respect to the *tbT* facies and, consequently, greater turbulence in the parental flow. Load-driven soft deformation supports this interpretation, indicating water saturation in the deposit. Despite this, the internal fabric of the *tsT* facies, dominated by parallel horizontal stratification, leads us to infer deposition from hyperconcentrated flows transitional to streamflow (Fig. 6).

We interpret the *tsT/tbT* facies association as representing the head and tail (*tsT* facies) of ash-rich hyperconcentrated flash flood events (*tbT* facies). The relatively higher proportion of "local" epiclastic material in the *tsT* facies further supports its interpretation as the waxing and waning phases of these flows (Fig. 6; Vallance and Iverson, 2015). We interpret the occurrence of the *tsT* facies interbedded within the *tbT* facies as evidence of successive mass flow surges. Additionally, the good preservation of glass shards and, in general, a low degree of epiclastic contamination, suggest remobilization during a short-lived torrential event, rather than long-term ash reworking (e.g., by pyroclastic-rich dunes or large fluvial systems). Ash remobilization by torrential mass flows likely occurred shortly after primary sedimentation and subsequent epiclastic deposits quickly buried the remobilized ash.

5. Discussion

5.1. Hazard implications

Remobilization processes frequently affect distal tephra deposits from large eruptions due to their widespread distribution and the variety of depositional environments in which they accumulate. Unlike the immediate primary hazards associated with an eruption, tephra remobilization represents a secondary hazard that can persist over extended timescales. Identifying the key mechanisms of tephra remobilization following past eruptions is essential for understanding the post-eruptive evolution of cascading hazardous phenomena in the distal environment.

Previous studies interpreted the *tsT* facies as primary fall deposits, with the observed stratification attributed to instabilities in the eruptive column (facies $CB_2$1; Fernández-Turiel et al., 2019). Similarly, the *tbT* facies was also interpreted as primary fall deposits generated during a phase of the eruption characterized by a more stable column (facies $CB_2$2; Fernández-Turiel et al., 2019). Additionally, the presence of anomalous several-meter-thick fall deposits located hundreds of kilometers from the CBVC (e.g., site CBT7; Fig. 3C) was attributed to particle aggregation within the volcanic plume or to turbulent perturbations induced by topography (Fernández-Turiel et al., 2019). However, both the *tsT* and *tbT* facies exhibit internal features compatible with deposition from mass flows. In addition, thickness variations, including valley-pond lenticular morphologies, along the drainage network of the Tafí Valley (Fig. 2B) strongly suggest over-thickening caused by remobilization of primary fallout deposits due to mass flow processes (Fig. 6). Thus, the ash-rich hyperconcentrated mass flows described here can be defined as secondary "distal lahars" (e.g., Córdoba et al., 2015; Mulas et al., 2019). Lahars are highly energetic events involving the remobilization of loose volcanic material by debris flows and hyperconcentrated flows (Pierson et al., 1990, 1992; Smith and Lowe, 1991; Lavigne et al., 2000; Witham, 2005; Manville et al., 2009; De Bélizal et al., 2013; Pistolesi et al., 2013; Pierson and Major, 2014). Primary lahars are directly triggered by eruptive events, typically through the catastrophic drainage of crater lakes or the interaction of PDCs with snow or ice (e.g., Pierson et al., 1990; Manville and Cronin, 2007). In contrast, secondary lahars result from the remobilization of loose pyroclastics, usually triggered by heavy rainfall (e.g., Pierson et al., 1992; Capra et al., 2010; De Bélizal et al., 2013; Charbonnier et al., 2018).

While lahars are commonly associated with volcanic slopes, "distal lahars" can also develop in surrounding mountainous regions, sometimes hundreds of kilometers from the source (Córdoba et al., 2014; Mulas et al., 2019). Immediately following large eruptions, freshly deposited ash typically causes a sharp reduction in soil permeability, leading to increased surface runoff, erosion, and sediment mobilization (Yamakoshi et al., 2005; Manville et al., 2009; Pierson and Major, 2014; Baumann et al., 2020). This rapid landscape alteration is especially evident in regions with steep terrain or intense rainfall. Ash remobilization is often initiated by rill and sheet erosion, as well as by shallow landslides, usually during the first significant rainfall following the eruption (Baumann et al., 2020). These processes can quickly strip the surface of its fine ash mantle and transport large volumes of sediment downslope into river systems, altering sediment budgets and geomorphic dynamics. The magnitude of rain-induced ash remobilization is controlled by various interrelated factors, including rainfall intensity, slope angle, grain size distribution, substrate hydraulic conductivity, and deposit thickness (Baumann et al., 2018, 2020).

The *tbT/tsT* facies association related to mass flow events appears to be a regionally conspicuous feature of the distal deposits from the Cerro Blanco eruption, especially in the Tafí Valley and surrounding areas (Figs. 2 and 5; figure 6 in Fernández-Turiel et al., 2019). Additionally, distal tephras associated with other Quaternary eruptions in northwestern Argentina also show evidence of mass flow remobilization shortly after deposition (e.g., Campo de la Piedra Pómez eruption; Báez et al., 2025). Hence, the generation of hyperconcentrated secondary lahars likely represents the most common mechanism of loose tephra remobilization in the intermontane valleys of northwestern Argentina.

In the southern Puna region, in contrast, wind remobilization plays a dominant role (e.g., de Silva et al., 2010, 2013; Mingari et al., 2017). Evidence of long-term wind remobilization of tephra from the ~4.2 ka BP Cerro Blanco eruption is still visible in the Fiambalá Valley, located south of the CBVC (Mingari et al., 2017). Furthermore, prolonged aeolian remobilization following the eruption likely played a significant role in altering hunter-gatherer settlement patterns in northwestern Argentina (Carbonelli et al., 2022).

Our results highlight the importance of hyperconcentrated mass flows as a key mechanism of ash remobilization immediately after the eruption. While the dynamics and hazard implications of wind-induced ash resuspension and proximal primary or secondary lahars have been extensively studied worldwide, widespread secondary “distal lahars” triggered by large Plinian eruptions remain underexplored (e.g., Córdoba et al., 2015), representing an overlooked volcanic hazard in northwestern Argentina and in other volcanically active regions.

5.2. Implications for future tephrochronological and volcanological research

Despite evidence of remobilization recorded in facies *tbT* and *tsT* (internal structures and local overthickening), our results show a relatively homogeneous glass shard-rich componentry with well-preserved primary textures, suggesting that reworking was limited in extent and likely occurred shortly after deposition. Consequently, while these deposits may not be suitable for ultra-high-resolution tephrochronological analyses, they can still offer valuable chronostratigraphic information (Lowe, 2011). This makes them particularly useful for volcanological, stratigraphic, neotectonic, geoarchaeological, and paleoclimatic studies (Sampietro-Vattuone and Peña-Monné, 2016; Peña Monné and Sampietro-Vattuone, 2018).

Given the extensive spatial distribution of the fall deposits from the Cerro Blanco eruption, we agree that it probably ranks among the most significant Holocene volcanic events in the Andes, and even possibly on a global scale. We, however, caution that our reinterpretation of the *tbT/tsT* facies association as remobilized fallout deposits raises important questions about the volume and VEI estimates of the Cerro Blanco eruption presented in earlier studies (Fernández-Turiel et al., 2019). As we discussed above, many of the outcrops used for those estimates show clear evidence of remobilization (see figure 6 in Fernández-Turiel et al., 2019). We therefore propose that a revised volume estimation is needed, based on a detailed reassessment of the most relevant outcrops to confirm that only primary deposits are being considered (e.g., Buckland et al., 2020).

6. Conclusions

A comprehensive facies analysis of the distal tephra deposits associated with the ~4.2 ka BP Cerro Blanco eruption, combined with a review of existing literature, indicates that most of these deposits resulted from remobilization by rain-triggered hyperconcentrated flows, which can be classified as secondary "distal lahars". This process appears to be an overlooked volcanic hazard in northwestern Argentina. The compositional, textural, and granulometric similarity of these deposits to layers considered primary fall deposits suggest that remobilization was likely localized and occurred shortly after the eruption. Consequently, the distal tephra deposits related to the Cerro Blanco eruption remain tephrochronologically reliable; however, their use for estimating eruptive source parameters (e.g., eruption volume) should be carefully evaluated on an outcrop-by-outcrop basis to discard remobilized material.

Acknowledgments

This work has been supported by the US National Science Foundation grant EAR 2243737. We also thank Agustin Ortiz for his enthusiastic support during the fieldwork. Finally, we would like to thank Dr. Daniel Bertin for his meticulous editorial work, as well as Dr. Andrea Di Capua and an anonymous reviewer for their constructive comments and valuable suggestions, which significantly improved this manuscript.

References

Báez, W.; Arnosio, M.; Chiodi, A.; Ortiz Yañes, A.; Viramonte, J.G.; Bustos, E.; Giordano, G.; López J. F. 2015. Estratigrafía y evolución del Complejo Volcánico Cerro Blanco, Puna Austral, Argentina. Revista Mexicana de Ciencias Geológicas,32 (1): 29-49.

Báez, W. A.; Chiodi, A. L.; Bustos, E.; Arnosio, J. M.; Viramonte, J. G.; Giordano, G.; Alfaro Ortega, B. B. 2017. Mecanismos de emplazamiento y destrucción de los domos lávicos asociados a la caldera del Cerro Blanco, Puna Austral. Revista de la Asociación Geológica Argentina, 74 (2): 223-238.

Báez, W.; Bustos, E.; Chiodi, A.; Reckziegel, F.; Arnosio, M.; de Silva, S.; Giordano, G.; Viramonte, J.G.; Sampietro-Vattuone, M.M.; Peña-Monné J.L. 2020a. Eruptive style and flow dynamics of the pyroclastic density currents related to the Holocene Cerro Blanco eruption (Southern Puna plateau, Argentina). Journal of South American Earth Sciences 98: 102482

Báez, W.; de Silva, S.; Chiodi, A.; Bustos, E.; Giordano, G.; Arnosio, M.; Suzaño, N.; Viramonte, J.G.; Norini, G.; Groppelli, G. 2020b. Pulsating flow dynamics of sustained, forced pyroclastic density currents: insights from a facies analysis of the Campo de la Piedra Pómez ignimbrite, southern Puna, Argentina. Bulletin of volcanology, 82: 1-32.

Báez, W.; Bardelli, L.; Sampietro-Vattuone, M. M.; Monné, J. P.; Bertea, E.; and Cirer, M. 2024. Revisiting the Holocene tephrochronology of northwestern Argentina: Insights from geochemical characterization of the tephras from the Tafí valley. Journal of South American Earth Sciences, 134: 104745.

Báez, W.; de Silva, S.; Cirer, M.; Bertea, E.; Constantinescu, R.; Danišík, M.; Schmitt, A.K.; Ramos F. 2025. Dynamics of one of the largest Quaternary explosive eruptions in the Andes: The ca. 29 ka Campo de la Piedra Pómez VEI ≥6 caldera-forming eruption, NW Argentina. Bulletin of Volcanology. In press.

Baumann, V.; Bonadonna, C., Cuomo, S.; Moscariello, M.; Manzella, I. 2018. Slope stability models for rainfall-induced lahars during long-lasting eruptions. Journal of Volcanology and Geothermal Research, 359: 78-94.

Baumann, V.; Bonadonna, C.; Cuomo, S.; Moscariello, M. 2020. Modelling of erosion processes associated with rainfall-triggered lahars following the 2011 Cordon Caulle eruption (Chile). Journal of Volcanology and Geothermal Research, 390: 106727.

Blott, S. J.; Pye, K. 2001. GRADISTAT: a grain size distribution and statistics package for the analysis of unconsolidated sediments. Earth surface processes and Landforms, 26(11): 1237-1248.

Boretto, G.; Zanchetta, G.; Bini, M.; Cioccale, M.; Carignano, C.; Gordillo, S.; Giaccio B.; Fernández Turiel J.L.; Arienzo I.; Isola, I. 2021. Cerro Blanco 4.2 ka volcanic ash deposit at Cerro Colorado (Córdoba Province, Argentina). Comitato Glaciologico Italiano; Geografia Fisica e Dinamica Quaternaria; 44; 13 (4): 173-181

Branney, M. J.; Kokelaar, B. P. 2002. Pyroclastic density currents and the sedimentation of ignimbrites. Geological Society of London.

Buckland, H. M.; Cashman, K. V.; Engwell, S. L.; Rust, A. C. 2020. Sources of uncertainty in the Mazama isopachs and the implications for interpreting distal tephra deposits from large magnitude eruptions. Bulletin of Volcanology, 82(3): 23.

Capra, L.; Borselli, L.; Varley, N.; Gavilanes-Ruiz, J. C.; Norini, G.; Sarocchi, D.; Caballero L.; Cortes, A. 2010. Rainfall-triggered lahars at Volcán de Colima, Mexico: surface hydro-repellency as initiation process. Journal of Volcanology and Geothermal Research, 189(1-2): 105-117.

Carbonelli, J. P.; Fernandez-Turiel, J. L.; de Medina, C. B. L. 2022. The Abra del Toro rock shelter, northwestern Argentina, a space occupied by hunter-gatherers that was hit by the large 4.2 ka Cerro Blanco eruption. Journal of Archaeological Science: Reports, 45: 103629.

Castruccio, A.; Clavero, J.; Rivera, A. 2010. Comparative study of lahars generated by the 1961 and 1971 eruptions of Calbuco and Villarrica volcanoes, Southern Andes of Chile. Journal of Volcanology and Geothermal Research, 190(3-4): 297-311.

Charbonnier, S. J.; Connor, C. B.; Connor, L. J.; Sheridan, M. F.; Oliva Hernández, J. P.; Richardson, J. A. 2018. Modeling the October 2005 lahars at Panabaj (Guatemala). Bulletin of Volcanology, 80: 1-16.

Chiodi, A.; Tassi, F.; Báez, W.; Filipovich, R.; Bustos, E., Galli, M.G.; Suzaño, N.; Ahumada, M.F.; Viramonte, J.G.; Giordano, G.; Pecoraino, G.; Vaselli, O. 2019. Preliminary conceptual model of the Cerro Blanco caldera-hosted geothermal system (Southern Puna, Argentina): Inferences from geochemical investigations. Journal of South American Earth Sciences, 94: 102213.

Cioni, R.; Pistolesi, M.; Rosi, M. 2015. Plinian and subplinian eruptions. In The Encyclopedia of Volcanoes (Sigurdsson, H.; editor). Academic press: 519-535. Amsterdam.

Córdoba, G.; Villarosa, G.; Sheridan, M. F.; Viramonte, J. G.; Beigt, D.; Salmuni, G. 2015. Secondary lahar hazard assessment for Villa la Angostura, Argentina, using Two-Phase-Titan modelling code during 2011 Cordón Caulle eruption. Natural Hazards and Earth System Sciences, 15(4): 757-766.

Cortés–Jiménez, G.P. 2020. Holocene lahar deposits associated with the eruptive activity of Cerro Machín Volcano, Colombia: Impact on landscape and associated potential hazard. In: Gómez, J. & Pinilla–Pachon, A.O. (editors), The Geology of Colombia, Volume 4 Quaternary. Servicio Geológico Colombiano, Publicaciones Geológicas Especiales 38, p. 297–331. Bogotá.

De Bélizal, E.; Lavigne, F.; Hadmoko, D. S.; Degeai, J. P.; Dipayana, G. A.; Mutaqin, B. W.; Vidal, C. 2013. Rain-triggered lahars following the 2010 eruption of Merapi volcano, Indonesia: A major risk. Journal of Volcanology and Geothermal Research, 261: 330-347.

de Silva, S. 2010. The largest wind ripples on Earth: Comment. Geology, 38(9): e218-e218.

de Silva, S. L.; Bailey, J. E.; Mandt, K. E.; Viramonte, J. M. 2010. Yardangs in terrestrial ignimbrites: Synergistic remote and field observations on Earth with applications to Mars. Planetary and Space Science, 58(4): 459-471.

de Silva, S. L.; Spagnuolo, M. G.; Bridges, N. T.; Zimbelman, J. R. 2013. Gravel-mantled megaripples of the Argentinean Puna: A model for their origin and growth with implications for Mars. Bulletin, 125(11-12): 1912-1929.

de Silva, S. L.; Roberge, J.; Bardelli, L.; Báez, W.; Ortiz, A.; Viramonte, J. G.; Arnosio M.; Becchio, R. 2022. Magmatic evolution and architecture of an arc-related, rhyolitic caldera complex: The late Pleistocene to Holocene Cerro Blanco volcanic complex, southern Puna, Argentina. Geosphere, 18(2): 394-423.

Di Capua, A. D.; Rosa, R. D.; Kereszturi, G.; Pera, E. L.; Rosi, M.; Watt, S. F. L. 2023. Volcanically-derived deposits and sequences: a unified terminological scheme for application in modern and ancient environments. Geological Society, London, Special Publications, 520: 11-27.

Di Vito, M. A., Rucco, I., de Vita, S., Doronzo, D. M., Bisson, M., de' Michieli Vitturi, M., Rosi, M., Sandri, L., Zanchetta, G., Zanella, E., and Costa, A.: Lahar events in the last 2000 years from Vesuvius eruptions – Part 1: Distribution and impact on densely inhabited territory estimated from field data analysis, Solid Earth, 15, 405–436

Fernández-Turiel, J. L.; Perez–Torrado, F. J.; Rodríguez-González, A.; Saavedra, J.; Carracedo, J. C.; Rejas, M.; Lobo, A.; Osterrieth, M.; Carrizo, J. I.; Esteban, G.; Gallardo, J.; Ratto, N. 2019. The large eruption 4.2 ka cal BP in Cerro Blanco, Central Volcanic Zone, Andes: Insights to the Holocene eruptive deposits in the southern Puna and adjacent regions. Estudios Geológicos. v. 75 (1).

Folk, R. L.; Ward, W. C. 1957. Brazos River bar [Texas]; a study in the significance of grain size parameters. Journal of sedimentary research, 27(1): 3-26.

Froese, D.G.; Zazula, G.D.; Reyes, A.V. 2006. Seasonality of the late Pleistocene Dawson tephra and exceptional preservation of a buried riparian surface in central Yukon Territory, Canada. Quaternary Science Reviews 25: 1542–1551.

Galván, A.F. 1981. Descripción geológica de la Hoja 10e, Cafayate, Provincias de Tucumán, Salta y Catamarca. Escala 1:200.000. Servicio Geológico Nacional, Boletín 177. Servicio Geológico Nacional, Buenos Aires, Argentina.

Giordano, G.; Cas, R.; Wright, J. V. 2024. Explosive Eruption Styles, Columns, and Pyroclastic Fallout Deposits: Subaerial and Subaqueous, Dynamics, Deposit Characteristics and Classification. In Volcanology: Processes, Deposits, Geology and Resources (pp. 519-691). Cham: Springer International Publishing.

González, O.E. 1997. Geología de La Angostura, valle de Tafí, Tucuman. In: XIV Congreso Geológico Argentino, Salta, Argentina: 283–286.

Harpel, C.J.; de Silva, S.L.; Salas, G. 2011. The 2 ka Eruption of Misti Volcano, Southern Peru—The Most Recent Plinian Eruption of Arequipa's Iconic Volcano. GSA Special Papers. Volume 484.

Henderson, S.T.; Pritchard, M.E. 2013. Decadal volcanic deformation in the Central Andes Volcanic Zone revealed by InSAR time series: Geochemistry, Geophysics, Geosystems, v. 14: 1358–1374,

Hermanns, R. L.; Schellenberger, A. 2008. Quaternary tephrochronology helps define conditioning factors and triggering mechanisms of rock avalanches in NW Argentina. Quaternary International, 178(1): 261-275.

Hermanns, R.L.; Trauth, M.H.; Niedermann, S.; McWilliams, M.; Strecker, M.R. 2000. Tephrochronologic constraints on temporal distribution of large landslides in Northwest Argentina. Journal of Geology 108: 35–52.

Hermanns, R.L.; Niedermann, S.; Villanueva García, A.; Schellenberger, A. 2006. Rock avalanching in the NW Argentine Andes as result of complex interactions of lithologic, structural and topographic boundary conditions, climate change and active tectonics. In: Evans, S.G., Scarascia-Mugnozza, G., Strom, A., Hermanns, R.L. (Eds.), Massive Rock Slope Failure: New Models for Hazard Assessment. NATO Science Series. Kluwer, Dordrecht, the Netherlands, pp. 539–569.

Iverson, R. M. 2003. Gravity-driven mass flows. In: Nichols, G. Middleton, G. V. (ed.) 2003. Encyclopedia of sediments and sedimentary rocks, 347-353. 821 pp. Dordrecht, Boston, London: Kluwer.

Janda, R. J.; Daag, A. S.; Delos Reyes, P. J.; Newhall, C. G.; Pierson, T. C.; Punongbayan, R. S.; Rodolfo, K.; Solidum, R.U.; Umbal, J. V. 1996. Assessment and response to lahar hazard around Mount Pinatubo, 1991 to 1993. Fire and mud: Eruptions and lahars of Mount Pinatubo, Philippines, 107-140.

Jenkins, S. F.; Wilson, T. M.; Magill, C.; Miller, V.; Stewart, C.; Blong, R.; Marzocchi W.; Boulton C.; Bonadonna C.; Costa, A. 2015. Volcanic ash fall hazard and risk. Global volcanic hazards and risk, 173-222.

Manville, V.; Cronin, S. J. 2007. Breakout lahar from New Zealand's crater lake. Eos, Transactions American Geophysical Union, 88(43): 441-442.

Manville, V.; Németh, K.; Kano, K. 2009. Source to sink: A review of three decades of progress in the understanding of volcaniclastic processes, deposits, and hazards. Sediment. Geol. 220: 136–161.

Manville, V.; Major, J. J.; Fagents, S. A. 2013. Modeling lahar behavior and hazards. Modeling volcanic processes: the physics and mathematics of volcanism, 300-330.

Mingari, L. A.; Collini, E. A.; Folch, A.; Báez, W.; Bustos, E.; Osores, M. S.; Reckziege, F.; Alexander, P.; Viramonte, J. G. 2017. Numerical simulations of windblown dust over complex terrain: the Fiambalá Basin episode in June 2015. Atmospheric Chemistry and Physics, 17(11): 6759-6778.

Montero-López, M.C.; Hongn, F.D.; Seggiaro, R.; Marrett, R.; Ratto, N. 2009. Relación entre el volcanismo y los registros arqueológicos en el bolsón de Fiambalá, en Ratto, N (ed.), Entrelazando ciencias, sociedad y ambiente antes de la conquista española: Buenos Aires, Editorial Eudeba, 131-156.

Montero-López, M.C.; Hongn, F.; Brod, J.A.; Seggiaro, R.; Marrett, R. and Sudo, M. 2010. Magmatismo ácido del Mioceno Superior-Cuaternario en el área de Cerro Blanco- La Hoyada, Puna Austral. Revista de la Asociación Geológica Argentina, 67: 329–348.

Mulas, M.; Chunga, K.; Garces Leon, D. O.; Escobar Segovia, K. F. 2019. Sedimentological study of distal rain-triggered lahars: The case of west coast of Ecuador. Latin American journal of sedimentology and basin analysis, 26(1): 1-17.

Newhall, C.; Self, S.; Robock, A. 2018. Anticipating future Volcanic Explosivity Index (VEI) 7 eruptions and their chilling impacts: Geosphere, v. 14: 572–603,

Lamberti, M.C.; Chiodi, A.; Agusto, M.; Filipovich, R.; Massenzio, A.; Báez, W.; Tassi, F.; Vaselli, O. 2021. Carbon dioxide diffuse degassing as a tool for computing the thermal energy release at Cerro Blanco Geothermal System, Southern Puna (NW Argentina). Journal of South American Earth Sciences, 105: 102833.

Lavigne, F.; Thouret, J. C.; Voight, B.; Suwa, H.; Sumaryono, A. 2000. Lahars at Merapi volcano, Central Java: an overview. Journal of volcanology and geothermal research, 100(1-4): 423-456.

Losano, N.; Villarosa, G.; Beigt, D.; Amat, P.; Cottet, J.; Outes, V. 2024. Hydrologic remobilisation of tephra-fall deposits: A sedimentological analysis throughout fluvio-lacustrine systems of North-West Patagonia. The Depositional Record, 10(5): 670-684.

Lowe, D. J. 2011. Tephrochronology and its application: a review. Quaternary Geochronology, 6(2): 107-153.

Paredes-Mariño, J.; Forte, P.; Alois, S.; Chan, K. L.; Cigala, V.; Mueller, S. B.; Poret, M.; Spanu, A.; Tomašek, I.; Tournigand, P.; Perugini, D.; Kueppers, U. 2022. The lifecycle of volcanic ash: advances and ongoing challenges. Bulletin of Volcanology, 84(5): 51.

Peña Monné, J. L.; Sampietro-Vattuone, M. 2018. Paleoambientes holocenos del valle de Tafí (Noroeste Argentino) a partir de registros morfosedimentarios y geoarqueológicos. Boletín Geoógico y Minero de España, 129(4): 671-691

Petrinovic, I.A.; D'Elia, L. 2018. Rocas Volcaniclásticas: Depósitos, Procesos y Modelos de Facies. Asociación Argentina de Sedimentología, 184 pp

Pierson, T. C.; Major, J. J. 2014. Hydrogeomorphic Effects of Explosive Volcanic Eruptions on Drainage Basins. Annual Review of Earth and Planetary Sciences, 42(1): 469–507.

Pierson, T. C.; Janda, R. J.; Thouret, J. C.; Borrero, C. A. 1990. Perturbation and melting of snow and ice by the 13 November 1985 eruption of Nevado del Ruiz, Colombia, and consequent mobilization, flow and deposition of lahars. Journal of Volcanology and Geothermal Research, 41(1): 17-66.

Pierson, T.C.; Janda, R.J.; Umbal, J. V; Daag, A S. 1992. Immediate and long-term hazards from lahars and excess sedimentation in rivers draining Mount Pinatubo, Philippines. U.S. Geol. Surv. Water Resour. Invest. Rep: 92–403937.

Pistolesi, M.; Cioni, R.; Rosi, M.; Aguilera, E. 2014. Lahar hazard assessment in the southern drainage system of Cotopaxi volcano, Ecuador: Results from multiscale lahar simulations. Geomorphology, 207: 51-63.

Ratto, N. 2013. A modo de introducción: la articulación de estudios arqueológicos, paleoambientales e históricos en el oeste tinogasteño (Catamarca). In: Delineando prácticas de la gente del pasado: Los procesos socio-históricos del oeste catamarqueño (Ratto, N., ed.). Sociedad Argentina de Antropología, Buenos Aires, 17–44.

Robock, A. 2000. Volcanic eruptions and climate. Reviews of geophysics, 38(2): 191-219

Ruiz Huidobro, O.J. 1972. Descripción Geológica de la hoja 11e, Santa María, Provincias de Catamarca y Tucumán. Servicio Nacional Minero Geológico, Boletín 134. Servicio Nacional Minero Geológico, Buenos Aires, Argentina.

Sampietro-Vattuone, M. M.; Peña-Monné, J. L. 2016. Geomorphological dynamic changes during the Holocene through ephemeral stream analyses from Northwest Argentina. Catena, 147:663-677.

Sampietro-Vattuone, M.M., Peña-Monné, J.L., 2019. Geomorphology of Tafí valley (Tucumán Province, Northwest Argentina). Journal of Maps 15(2), 177–184.

Sampietro-Vattuone, M.M.; Báez, W.; Peña-Monné, J.L.; Sola A. 2020. Chronological and geomorphological approach to the Holocene tephras from Tafí and Santa María valleys, NWArgentina. Quaternary Research 94: 14-30.

Seggiaro, R.; Hongn, F.; Folguera, A.; Clavero, J. 2006. Hoja geológica 2769-II, paso de San francisco: instituto de Geología y recursos minerales, servicio geológico minero argentino. Boletín 294 (76).

Smith, G. A.; Lowe, D. R. 1991. Lahars: volcano-hydrologic events and deposition in the debris flow—hyperconcentrated flow continuum. In: Fisher, R.V. and Smith, G.A. (eds) Sedimentation in Volcanic Settings. SEPM Society for Sedimentary Geology, volume 45.

Sohn, Y. K. 1997. On traction-carpet sedimentation. Journal of Sedimentary Research, 67(3): 502-509.

Sohn, C., and Sohn, Y. K. 2019. Distinguishing between primary and secondary volcaniclastic deposits. Scientific Reports, 9(1), 12425.

Toselli, A.J.; Rossi, D.; Toselli, J.N.; Rapela, C.W. 1978. El basamento metamórfico de la Sierra de Quilmes, República Argentina. Revista de la Asociación Geológica Argentina 33: 105–121

Vallance, J. W. 2005. Volcanic debris flows. Debris-flow hazards and related phenomena, 247-274.

Vallance, J.W. 2024. Lahars: Origins, Behavior and Hazards. In: Jakob, M., McDougall, S., Santi, P. (eds) Advances in Debris-flow Science and Practice. Geoenvironmental Disaster Reduction. Springer, Cham.

Vallance, J. W.; Iverson, R. M. 2015. Lahars and their deposits. In The encyclopedia of volcanoes (Sigurdsson, H.; editor). Academic Press: 649-664. Amsterdam

Vélez, M.L.; Bustos, E.; Euillades, L.; Blanco, M.; López, J.F.S.; Barbero, I.; Berrocoso, M.; Martinez, A.G.; Viramonte, J.G. 2021. Ground deformation at the Cerro Blanco caldera: A case of subsidence at the Central Andes BackArc. Journal of South American Earth Sciences, 106: 102941.

White, J. D.; Houghton, B. F. 2006. Primary volcaniclastic rocks. Geology, 34(8): 677-680.

Witham, C.S. 2005. Volcanic disasters and incidents: a new database. J. Volcanol. Geotherm. Res. 148: 191-233.

Wilson, L.; Sparks, R.S.J.; Walker, G.P.L. 1980. Explosive volcanic eruptions — IV. The control of magma properties and conduit geometry on eruption column behaviour: Geophysical Journal of the Royal Astronomical Society, v. 63: 117–148

Yamakoshi, T.; Doi Y.; Osanai N. 2005. Post-eruption hydrology and sediment discharge at the Miyakejima volcano, Japan. Z. Geomorph. N.F., Suppl.-Vol. 140: 55-72. Berlin-Stuttgart.

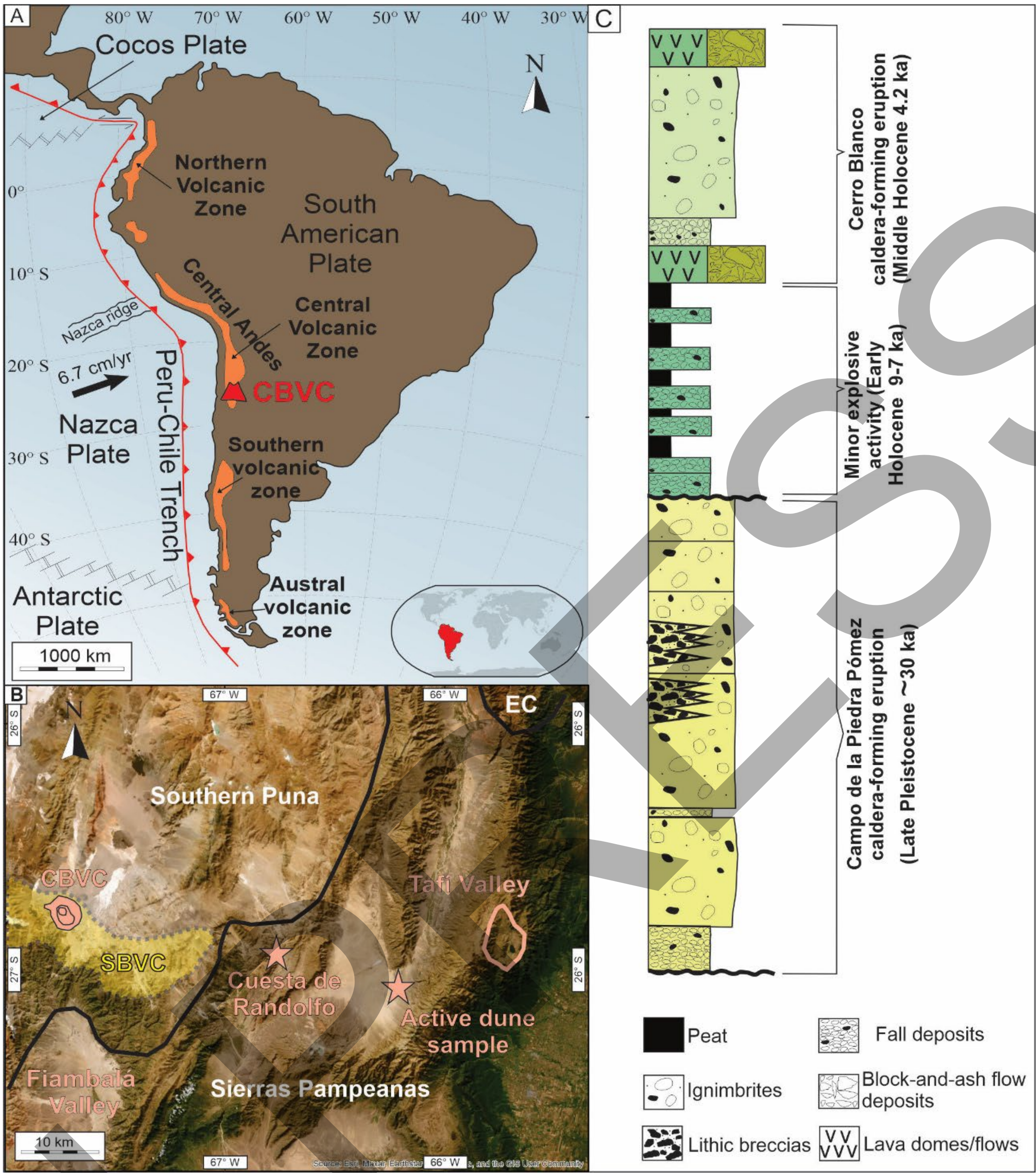

Fig. 1. A. Location of the Central Volcanic Zone (CVZ) and the Cerro Blanco Volcanic Complex (CBVC) within the geodynamic framework of South America. **B.** Location of the intermontane Tafí Valley within the geological provinces of northwestern Argentina. SBVC: San Buenaventura Volcanic Chain; EC: Eastern Cordillera. Pink stars indicate additional sampling and/or observation sites referred to in the text. **C.** Simplified stratigraphy of the CBVC (modified from Báez et al., 2015, and de Silva et al., 2022).

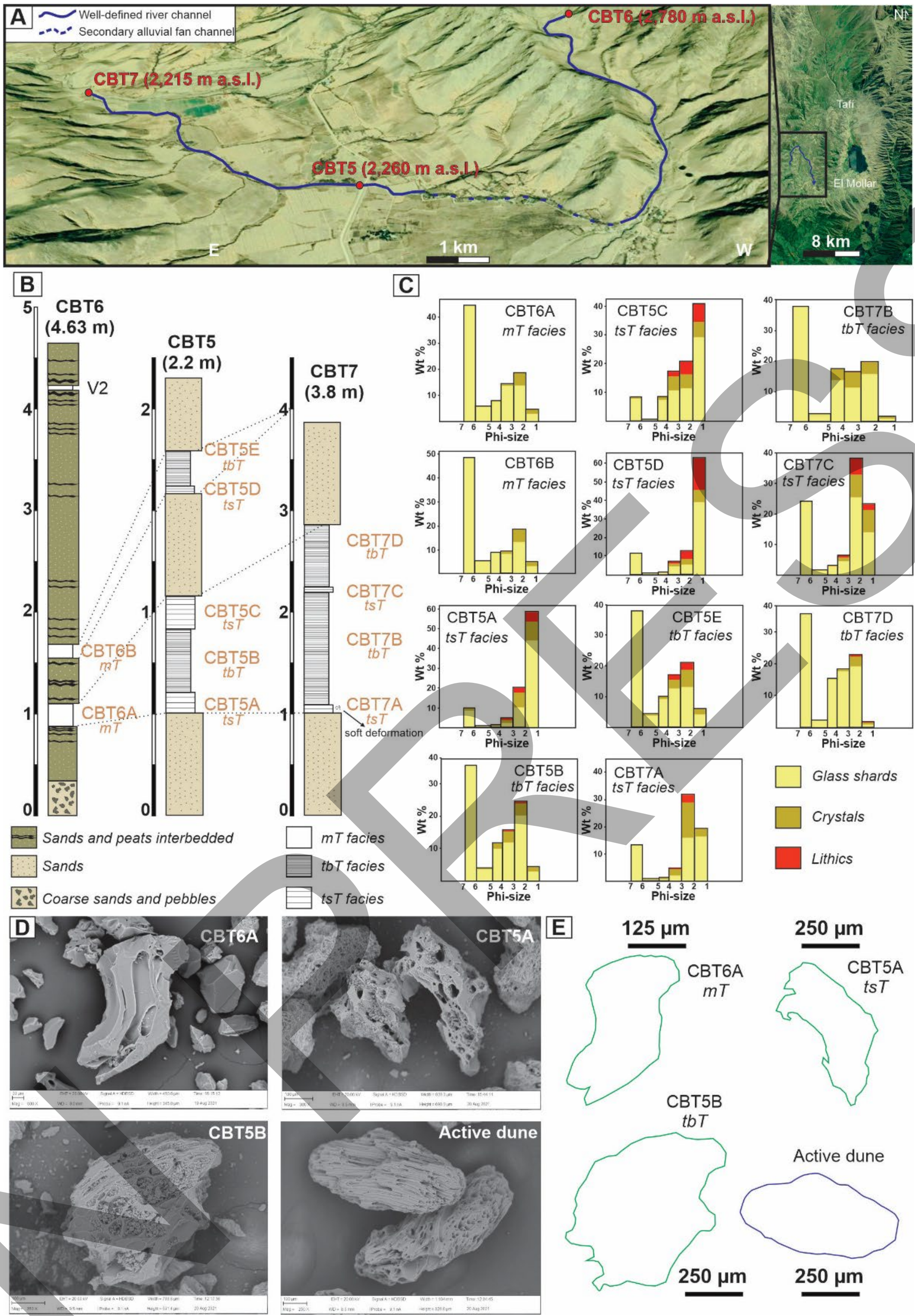

Fig. 2. A. Holocene sections along the drainage network of the Tafí Valley described in this paper. **B.** Stratigraphic profiles showing lateral changes in facies associations and thicknesses along the drainage network. V2: Upper Holocene ash described by Sampietro-Vattuone et al. (2020), unrelated to the Cerro Blanco Volcanic Complex. **C.** Grain size and componentry of the tephra layers present in the stratigraphic profiles. **D-E.** Scanning electron microscopy images (**D**) and interpreted sketches (**E**) of vitric shards (green outlines) from the facies recognized in the field. Note the comparison of micro-pumice morphology (blue outline) from an active pyroclast-rich dune (sample location in figure 1B). Note that in the detailed map in **A**, north is oriented toward the bottom of the panel.

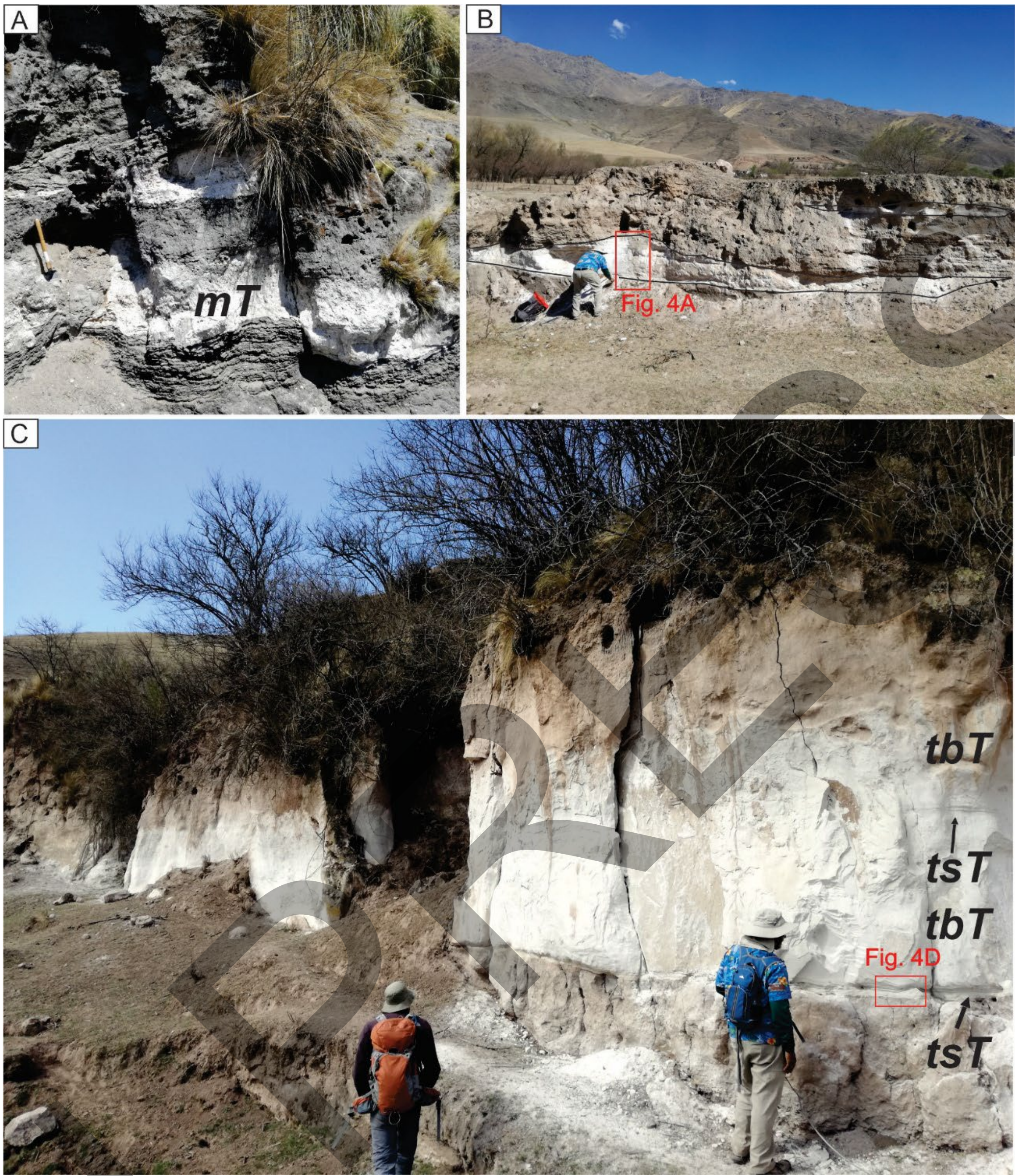

Fig. 3. Field view of the three sections studied in the Tafí Valley area. **A.** CBT6. **B.** CBT5. **C.** CBT7. *mT*: Massive Tuff facies; *tbT*: Thin-bedded Tuff facies; *tsT*: Thin-stratified Tuff facies.

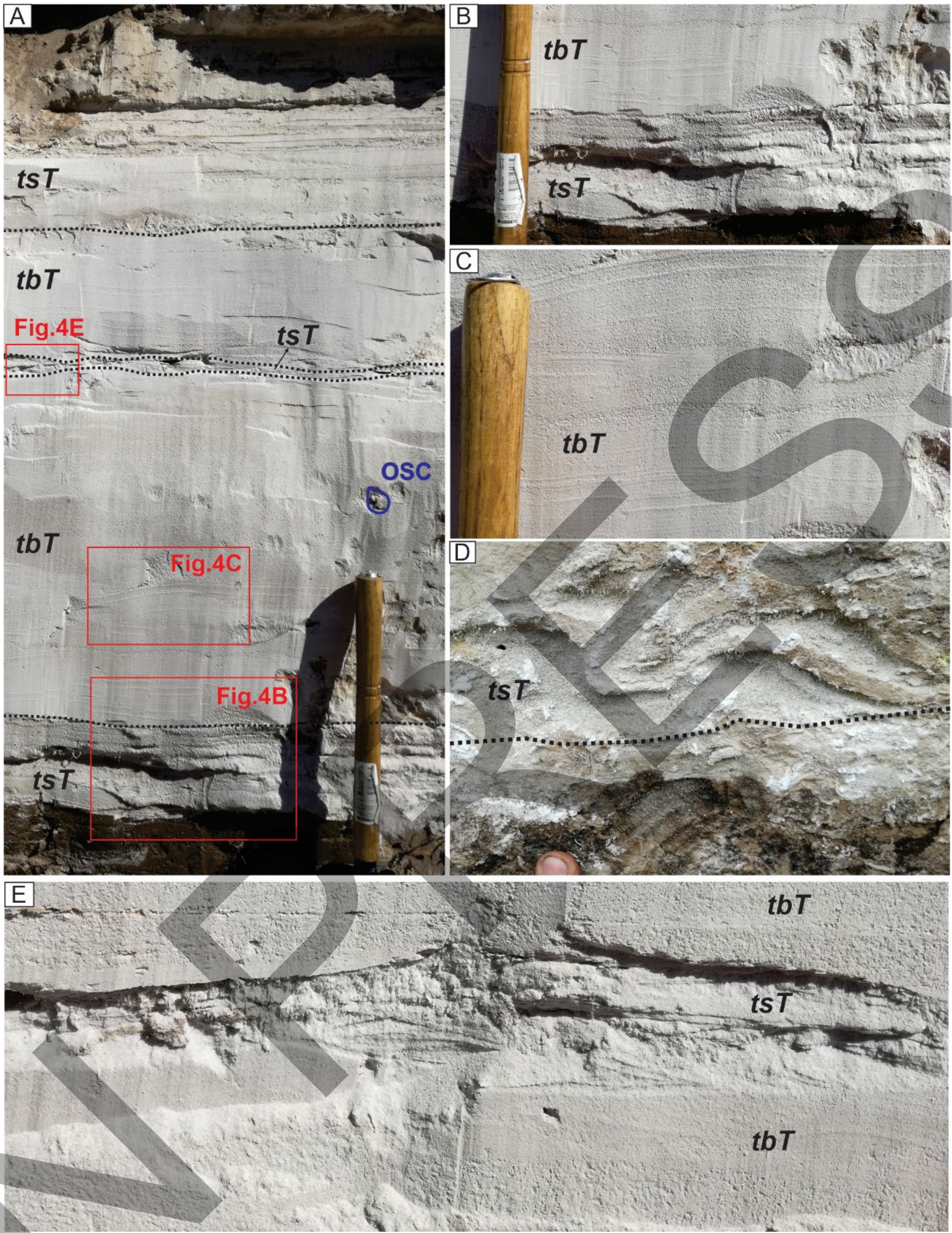

Fig. 4. Internal features and stratigraphic relationships of the thin-bedded Tuff (*tbT*) and the thin-stratified Tuff (*tsT*) facies. **A.** Example of the three different positions in which the *tsT* facies appears in relation to the *tbT* facies. The *tsT* facies is always present at the base of the *tbT* facies and occasionally at the top. Both facies interbedded are a far less frequent occurrence. Note the outsized lithic clast (OSC, blue outline) in the *tbT* facies. **B.** Thin bedding generated by alternating coarse and fine ash in the *tbT* facies and alternating, parallel, thin beds of coarse ash/scarce lapilli and fine to coarse ash in the *tsT* facies. **C.** Detail of the bedding in the *tbT* facies. **D.** Load-driven soft deformation indicating water saturation of the *tsT* facies. **E.** Truncation of individual layers and planar cross-stratification in the *tsT* facies. See figure 3B for section location.

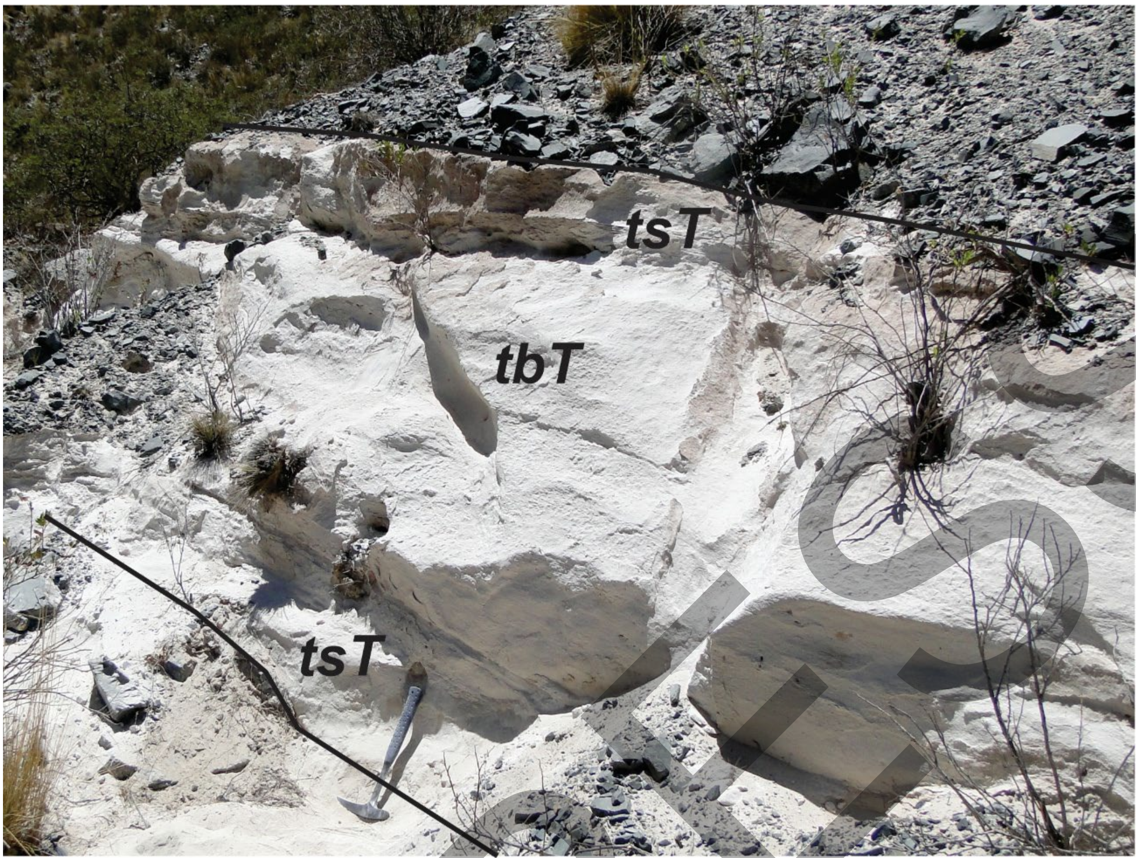

Fig. 5. Meter-thick outcrop at Cuesta de Randolfo (~80 km east of the Cerro Blanco Volcanic Complex; see location in figure 1B). Note the typical *tbT*/*tsT* facies association, inferred as a hyperconcentrated flow deposit (secondary "distal lahar").

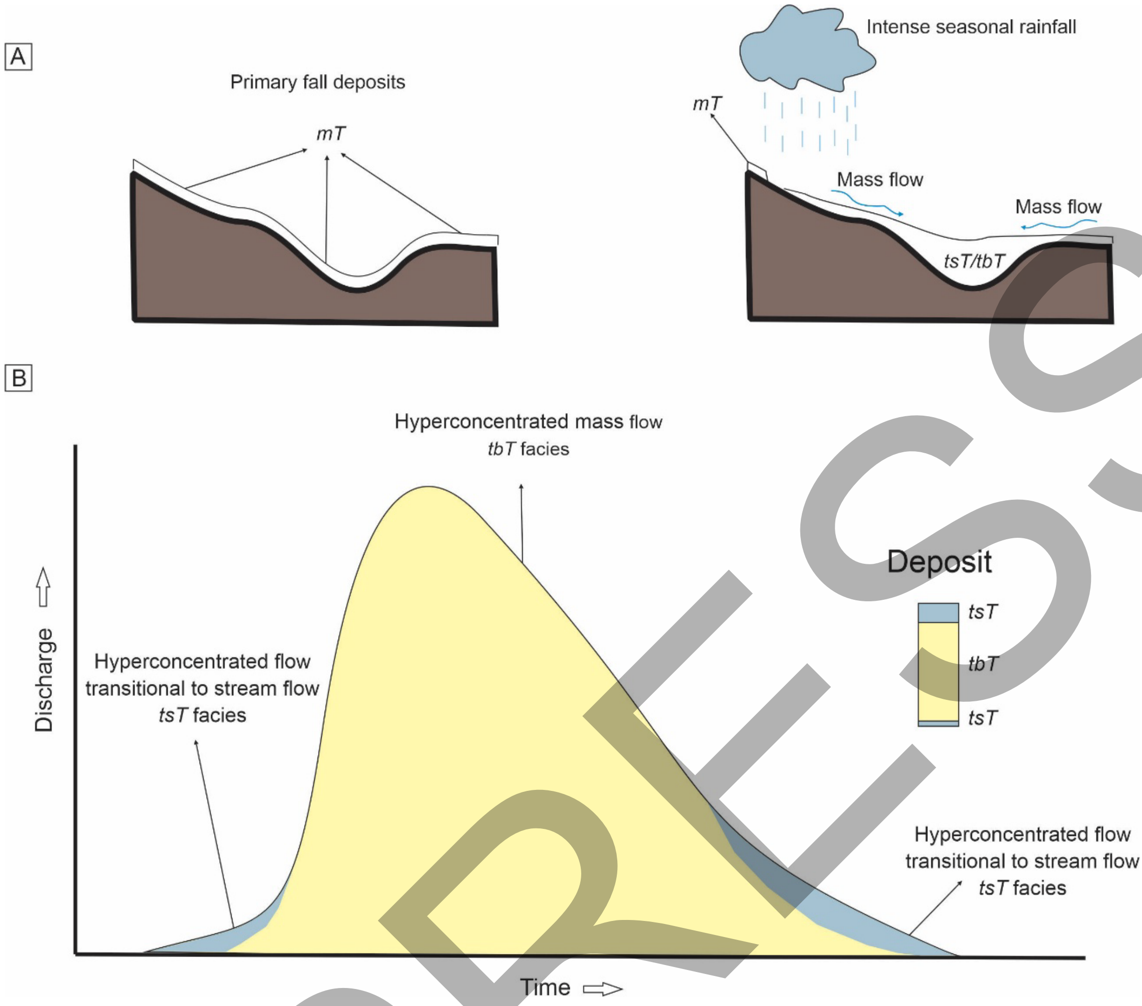

Fig. 6. A. Conceptual model based on Vallance and Iverson (2015) of the main processes behind the remobilization of distal fall deposits in the Tafí Valley area, shortly after the ~4.2 ka BP Cerro Blanco eruption. **B.** Flow dynamics and deposit architecture of secondary "distal lahars".